

Nuclear dependence of $R = \frac{\sigma_L}{\sigma_T}$ and Callan-Gross relation in nuclei

F. Zaidi,¹ H. Haider,¹ M. Sajjad Athar*,¹ S. K. Singh,¹ and I. Ruiz Simo²

¹*Department of Physics, Aligarh Muslim University, Aligarh - 202002, India*

²*Departamento de Física Atómica, Molecular y Nuclear,*

and Instituto de Física Teórica y Computacional Carlos I, Universidad de Granada, Granada 18071, Spain

The electromagnetic nuclear structure functions $F_{1A}(x, Q^2)$, $F_{2A}(x, Q^2)$ and $F_{LA}(x, Q^2)$ have been calculated using a microscopic model of nucleus to study the nuclear medium effects on the ratio $R_A(x, Q^2) = \frac{\sigma_{LA}(x, Q^2)}{\sigma_{TA}(x, Q^2)} = \frac{F_{LA}(x, Q^2)}{2xF_{1A}(x, Q^2)}$ and the Callan-Gross relation (CGR) in nuclei. The nuclear medium effects due to the Fermi motion, binding energy, nucleon correlations, mesonic contribution and shadowing have been taken into account. The theoretical results for the nuclear dependence of $R_A(x, Q^2)$ and its impact on CGR have been presented and compared with the available experimental data on the various nuclear targets. The predictions have been made for $R_A(x, Q^2)$ in the kinematic region of x and Q^2 for some nuclei relevant for the future experiments to be performed at the JLab.

PACS numbers: 13.40.-f, 13.60.-r, 21.65.-f, 24.85.+p

I. INTRODUCTION

A better theoretical understanding of the nuclear medium effects in the deep inelastic scattering (DIS) region in the electromagnetic (EM) and weak interaction induced processes has been emphasized [1–5] in view of the present DIS experiments being performed on various nuclear targets using the electron beams at the JLab [6–9] and the neutrino/antineutrino beams at the Fermilab [10]. A dedicated experiment at the JLab to study the nuclear medium effects in the kinematic region of $Q^2 (1 < Q^2 < 5 \text{ GeV}^2)$ and $x (0.1 < x < 0.6)$ for the electron induced DIS process on hydrogen, deuterium, carbon, copper and gold targets has been proposed [9]. Nuclear medium effects are also being studied in the $\nu_l/\bar{\nu}_l$ -nucleus scattering in the nuclear targets like carbon, iron and lead in the MINER ν A experiment at the Fermilab [11]. Generally, the experimental results of the cross section for DIS processes induced by the charged leptons and the neutrinos/antineutrinos on the nucleons and the nuclear targets are interpreted in terms of the structure functions. In the case of EM DIS processes induced by the leptons on the nucleons, the cross sections are described in terms of the two nucleon structure functions $F_{1N}(x, Q^2)$ and $F_{2N}(x, Q^2)$, where $x (= \frac{Q^2}{2M_N\nu})$ is the Bjorken scaling variable, M_N is the mass of target nucleon, $\nu (= E - E')$ and $Q^2 (= 4EE' \sin^2(\frac{\theta}{2}))$ are the energy and four momentum transfer square to the hadronic system. The structure function $F_{1N}(x, Q^2)$ describes the contribution of the transverse component of the virtual photon to the DIS cross sections while the structure function $F_{2N}(x, Q^2)$ describes a linear combination of the longitudinal and transverse components. Alternately, the DIS cross section is also described in terms of the transverse structure function $F_{TN}(x, Q^2)$ and the longitudinal structure function $F_{LN}(x, Q^2)$ defined as

$$F_{TN}(x, Q^2) = 2xF_{1N}(x, Q^2); \quad F_{LN}(x, Q^2) = \left(1 + \frac{4M_N^2x^2}{Q^2}\right) F_{2N}(x, Q^2) - 2xF_{1N}(x, Q^2). \quad (1)$$

The transverse and longitudinal cross sections are then expressed as

$$\sigma_{TN, LN}(x, Q^2) = \left(\frac{4\pi^2\alpha}{2x\nu(1-x)M_N}\right) F_{TN, LN}(x, Q^2). \quad (2)$$

The ratio of the purely longitudinal to transverse cross sections, $R_N(x, Q^2)$ is defined as

$$R_N(x, Q^2) = \frac{\sigma_{LN}(x, Q^2)}{\sigma_{TN}(x, Q^2)} = \frac{F_{LN}(x, Q^2)}{2xF_{1N}(x, Q^2)} = \left(1 + \frac{4M_N^2x^2}{Q^2}\right) R_{2N}(x, Q^2) - 1; \quad R_{2N}(x, Q^2) = \frac{F_{2N}(x, Q^2)}{2xF_{1N}(x, Q^2)}. \quad (3)$$

In the kinematic region of Bjorken scaling ($Q^2 \rightarrow \infty$, $\nu \rightarrow \infty$ such that $x = \frac{Q^2}{2M_N\nu} \rightarrow \text{constant}$), all the nucleon structure functions scale i.e. $F_{iN}(x, Q^2) \rightarrow F_{iN}(x)$ ($i = 1, 2, L$). In this kinematic region, the structure functions

* Corresponding author: sajathar@gmail.com

$F_{1N}(x)$ and $F_{2N}(x)$ calculated in the quark-parton model satisfy the Callan-Gross relation given by [12]:

$$F_{2N}(x) = 2xF_{1N}(x) \quad (4)$$

$$\text{implying } R_{2N}(x, Q^2) \rightarrow 1, \text{ and } R_N(x, Q^2) \rightarrow 0 \text{ in the limit of } Q^2 \rightarrow \infty. \quad (5)$$

Therefore, in the kinematic limit of the Bjorken scaling, the EM DIS data on the scattering of the electrons from the proton targets are analyzed in terms of only one structure function $F_{2N}(x)$. An explicit evaluation of $F_{2N}(x)$ in the quark parton model gives [13]:

$$F_{2N}(x) = 2xF_{1N}(x) = x \sum_i e_i^2 (f_i(x) + \bar{f}_i(x)), \quad (6)$$

where $f_i(x)$ and $\bar{f}_i(x)$ are the quark and antiquark parton distribution functions(PDFs) which describe the probability of finding a quark/antiquark of flavor i carrying a momentum fraction x of the nucleon's momentum. e_i^2 is the square of the charge corresponding to the quark/antiquark of flavor i .

As we move away from the kinematic region of the validity of Bjorken scaling towards the region of smaller Q^2 and ν , the description of structure function becomes more complex and the effects due to the target mass correction(TMC) and the higher twists(HT) as well as other non perturbative QCD effects arising due to the quark-quark and quark-gluon interactions are expected to give rise to Q^2 dependent contribution to the structure functions which violate scaling. Theoretical studies show that the corrections to the nucleon structure functions due to these effects decrease as $\frac{1}{Q^2}$, and therefore become important at small and moderate Q^2 [14–18]. These contributions may be different for $F_{1N}(x, Q^2)$ and $F_{2N}(x, Q^2)$ leading to the Q^2 dependent corrections in CGR given by Eqs.(4) and (5). There exist some phenomenological attempts to study the deviation of $R_N(x, Q^2)$ from its Bjorken limit by studying the Q^2 dependence of $F_{LN}(x, Q^2)$ in the region of smaller and moderate Q^2 [19–23]. These phenomenological studies describe the available experimental results on $R_N(x, Q^2)$ [19–27]. The most utilized parameterization of $R_N(x, Q^2)$ used in many experimental analyses is by Whitlow et al. [19].

In the case of nuclear targets the EM DIS cross sections are similarly analyzed in terms of nuclear structure function $F_{2A}(x, Q^2)$ assuming the validity of CGR at the nuclear level. A comparative study of nuclear structure function $F_{2A}(x, Q^2)$ with the free nucleon structure function $F_{2N}(x, Q^2)$ led to the discovery of the EMC effect [28, 29, 29]. The nuclear medium effects arising due to the Fermi motion, binding energy, nucleon correlations, shadowing, etc. in understanding the EMC effect, in the various regions of x has been extensively studied in the last 35 years [30–32].

However, there have been very few theoretical attempts to make a comparative study of the nuclear medium effects in $F_{LA}(x, Q^2)$, $F_{1A}(x, Q^2)$ and $F_{2A}(x, Q^2)$ and understand their implications on the modifications of $R_A(x, Q^2)$, $R_{2A}(x, Q^2)$ and CGR in nuclei. It has been argued that various nuclear medium effects arising due to the Fermi motion of nucleons, mesons, gluons distributions and higher twist effects in nuclei would contribute differently in the longitudinal and transverse structure functions in the various regions of x and Q^2 and induce nuclear dependence on $R_A(x, Q^2)$, $R_{2A}(x, Q^2)$ and CGR in nuclei [33–37]. Nuclear dependence of $R_A(x, Q^2)$ has been the topic of investigation in some experiments [23, 38–40] but no significant nuclear dependence has been reported. However, a reanalysis of these experiments shows a nontrivial nuclear dependence of $R_A(x, Q^2)$ and its implications on the extraction of the EMC ratio $\frac{F_{2A}(x, Q^2)}{F_{2D}(x, Q^2)}$ have been studied [2, 3]. In heavier nuclei, the Coulomb corrections to $R_A(x, Q^2)$ due to the initial and final electrons moving in the electrostatic potential $V(r)$ of the nucleus have also been considered and are found to be small and relevant only for DIS of the low energy electrons from the high Z nuclear targets [3]. The recent experimental measurements on the EM nuclear structure functions reported from the JLab on various nuclei in the kinematic region of $Q^2(1 < Q^2 < 5) \text{ GeV}^2$ and $x(0.1 < x < 1)$ also show that the nuclear medium effects are different for $F_{1A}(x, Q^2)$, $F_{2A}(x, Q^2)$ and $F_{LA}(x, Q^2)$ [6] and could modify the CGR in nuclei.

In view of these experimental results a comparative theoretical study of the nuclear structure functions $F_{iA}(x, Q^2)(i = 1, 2, L)$ for the electromagnetic processes and its effect on $R_A(x, Q^2)$, $R_{2A}(x, Q^2)$ and CGR in the nuclear medium in the various regions of x and Q^2 is highly desirable. A comparison of the theoretical results with the present and future experimental data from the JLab [6–9] will lead to a better understanding of the nuclear medium effects in EM structure functions.

In this work, we have studied the nuclear medium effects in the structure functions $F_{iA}(x, Q^2)$ ($i = 1, 2, L$) and nuclear dependence of $R_A(x, Q^2)$ in the regions of Q^2 and x relevant for the present and future experiments at the JLab in ^{12}C , ^{27}Al , ^{56}Fe , ^{63}Cu and ^{197}Au , assuming the Q^2 and x dependent phenomenological corrections to $R_N(x, Q^2)$ for the free nucleon case given by Whitlow et al. [19]. The impact of the nuclear dependence of $R_A(x, Q^2)$ on the CGR and its dependence on Q^2 has also been studied. In section II, the formalism for calculating the electromagnetic structure functions and the ratios $R_A(x, Q^2)$ and $R_{2A}(x, Q^2)$ in the nuclear medium is given in brief. In section III, the numerical results are presented which are summarized in section IV.

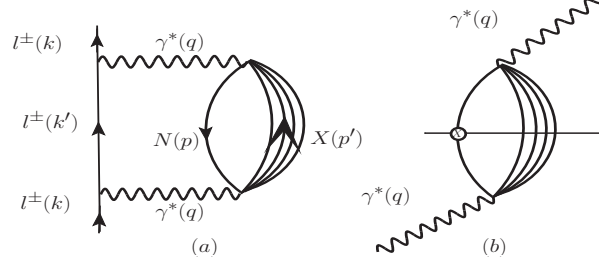


FIG. 1: Diagrammatic representation of (a) charged lepton self energy, (b) photon self energy with Cutkosky cuts(solid horizontal line) for putting particles on mass shell.

II. FORMALISM

In a nucleus, the charged lepton interacts with the nucleons which are moving with some momenta constrained by the Fermi momenta and Pauli blocking, and the nucleus is assumed to be at rest. Therefore, the free nucleon quark and antiquark PDFs should be convoluted with the momentum distribution of nucleons. In addition, there are binding energy corrections. Furthermore, the target nucleon being strongly interacting particle interacts with the other nucleons in the nucleus leading to the nucleon correlations effects. We have taken these effects into account by using a field theoretical model which starts with the Lehmann's representation for the relativistic nucleon propagator and the nuclear many body theory is used to calculate it for an interacting Fermi sea in the nuclear matter. A local density approximation is then applied to obtain the results for a finite nucleus. This technique results into the use of a relativistic nucleon spectral function that describes the energy and momentum distributions [41]. All the information like Fermi motion, binding energy and the nucleon correlations are contained in the spectral function. Moreover, we have considered the contributions of the pion and rho mesons in a many body field theoretical approach based on Refs. [42, 43]. The free meson propagator is replaced by a dressed one as these mesons interact with the nucleons in the nucleus through the strong interaction. We have earlier applied this model to study the nuclear medium effects in the electromagnetic and weak processes [5, 44], as well as proton induced Drell-Yan processes [45] on the nuclear targets.

In the case of a nuclear target, the expression for the differential scattering cross section is given by

$$\frac{d^2\sigma_A}{d\Omega dE'} = \frac{\alpha^2}{q^4} \frac{|\mathbf{k}'|}{|\mathbf{k}|} L_{\mu\nu} W_A^{\mu\nu}, \quad (7)$$

where α is the fine structure constant, $L_{\mu\nu} = 2(k_\mu k'_\nu + k'_\mu k_\nu - g_{\mu\nu} k \cdot k')$ is the leptonic tensor and $W_A^{\mu\nu}$ is the nuclear hadronic tensor which is expressed in terms of nuclear structure functions $W_{iA}(\nu, Q^2)$ ($i = 1, 2$) as

$$W_A^{\mu\nu} = W_{1A}(\nu, Q^2) \left(\frac{q^\mu q^\nu}{q^2} - g^{\mu\nu} \right) + \frac{W_{2A}(\nu, Q^2)}{M_A^2} \left(p_A^\mu - \frac{p_A \cdot q}{q^2} q^\mu \right) \left(p_A^\nu - \frac{p_A \cdot q}{q^2} q^\nu \right), \quad (8)$$

where M_A is the mass and p_A is the four momentum of the target nucleus.

The differential scattering cross section may also be written in terms of the probability per unit time (Γ) of finding a charged lepton interacting with a target nucleon given by [5]:

$$d\sigma = \Gamma dt dS = \Gamma \frac{dt}{dl} dl dS = \frac{\Gamma}{v} dV = \Gamma \frac{E(\mathbf{k})}{|\mathbf{k}|} dV = \frac{-2m_l}{|\mathbf{k}|} \text{Im}\Sigma(k) dV, \quad (9)$$

where dt is the time of interaction, dS is the differential area, dl and $v(= \frac{|\mathbf{k}|}{E(\mathbf{k})})$ stands for the length of interaction and velocity, respectively and dV is the volume element inside the nucleus. m_l is the lepton mass and $\text{Im}\Sigma(k)$ is the imaginary part of the lepton self energy (shown in Fig.1(a)) which is obtained by using the Feynman rules for the lepton self energy($\Sigma(k)$) given by

$$\Sigma(k) = ie^2 \int \frac{d^4q}{(2\pi)^4} \frac{1}{q^4} \frac{1}{2m_l} L_{\mu\nu} \frac{1}{k'^2 - m_l^2 + i\epsilon} \Pi^{\mu\nu}(q), \quad (10)$$

where $\Pi^{\mu\nu}(q)$ is the photon self energy which has been shown in Fig.1(b).

Using Eq.(10) in Eq.(9), the scattering cross section [42] is obtained as

$$\frac{d^2\sigma_A}{d\Omega dE'} = -\frac{\alpha}{q^4} \frac{|\mathbf{k}'|}{|\mathbf{k}|} \frac{1}{(2\pi)^2} L_{\mu\nu} \int \text{Im}[\Pi^{\mu\nu}(q)] d^3r \quad (11)$$

Now comparing Eq.(7) and Eq.(11), one may write the nuclear hadronic tensor $W_A^{\mu\nu}$ in terms of the photon self energy as:

$$W_A^{\mu\nu} = -\frac{1}{4\pi^2\alpha} \int Im[\Pi^{\mu\nu}(q)] d^3r \quad (12)$$

Using the Feynman rules, the expression for $\Pi^{\mu\nu}(q)$ is obtained as

$$\begin{aligned} \Pi^{\mu\nu}(q) = & e^2 \int \frac{d^4p}{(2\pi)^4} G(p) \sum_X \sum_{s_p, s_l} \prod_{i=1}^n \int \frac{d^4p'_i}{(2\pi)^4} \prod_l G_l(p'_l) \prod_j D_j(p'_j) \\ & < X | J^\mu | H > < X | J^\nu | H >^* (2\pi)^4 \delta^4(q + p - \sum_{i=1}^n p'_i), \end{aligned} \quad (13)$$

where G_l is the nucleon propagator and D_j is the meson propagator. In the above expression, $< X | J^\mu | H >$ is the hadronic current; s_p and s_l are respectively, the spins of nucleon and fermions in the final hadronic state X . $G(p)$ is the relativistic nucleon propagator inside the nuclear medium which is obtained using perturbative expansion of Dyson series in terms of the nucleon self energy (Σ^N) for an interacting Fermi sea. The nucleon self energy may be obtained using many body field theoretical approach in terms of spectral functions [41, 42]. Therefore, the nucleon propagator $G(p)$ inside the nuclear medium may also be expressed in terms of the particle and hole spectral functions as [41]:

$$G(p) = \frac{M_N}{E(\mathbf{p})} \sum_r u_r(\mathbf{p}) \bar{u}_r(\mathbf{p}) \left[\int_{-\infty}^{\mu} d\omega \frac{S_h(\omega, \mathbf{p})}{p_0 - \omega - i\eta} + \int_{\mu}^{\infty} d\omega \frac{S_p(\omega, \mathbf{p})}{p_0 - \omega + i\eta} \right], \quad (14)$$

where u and \bar{u} are respectively the Dirac spinor and its adjoint, $\mu \left(= \frac{p_F^2}{2M_N} + Re \left[\Sigma^N \left(\frac{p_F^2}{2M_N}, p_F \right) \right] \right)$ is the chemical potential and p_F is the Fermi momentum. S_h and S_p , respectively, stand for hole and particle spectral functions, the expression for which is taken from Ref. [41]. The spectral functions contain the information about the nucleon dynamics in the nuclear medium. All the parameters of the spectral function are determined by fitting the binding energy per nucleon and the Baryon number for each nucleus. Therefore, we are left with no free parameter. For more discussion please see Ref. [5, 42].

To obtain the contribution to the nuclear hadronic tensor $W_A^{\mu\nu}$, which is coming from the bound nucleons i.e. $W_{A,N}^{\mu\nu}$, due to the scattering of the charged leptons on the nuclear targets, we use Eq.(13) and Eq.(14) in Eq.(12), and express $W_{A,N}^{\mu\nu}$ in terms of the nucleonic tensor $W_N^{\mu\nu}$ convoluted over the hole spectral function S_h , and get

$$W_{A,N}^{\mu\nu} = 2 \sum_{\tau=p,n} \int d^3r \int \frac{d^3p}{(2\pi)^3} \frac{M_N}{E(\mathbf{p})} \int_{-\infty}^{\mu_\tau} dp_0 S_h^\tau(p_0, \mathbf{p}, \rho^\tau(r)) W_\tau^{\mu\nu}(p, q), \quad (15)$$

where $\rho^\tau(r)$ is the proton/neutron density inside the nucleus which is determined from the electron-nucleus scattering experiments and S_h^τ is the hole spectral function for the proton/neutron.

We take the zz component in Eq.(15) for $W_{A,N}^{\mu\nu}$ and $W_\tau^{\mu\nu}$, the momentum transfer \mathbf{q} along the z -axis, and using $F_{2N}(x) = \nu W_{2N}(\nu, Q^2)$, we obtain $F_{2A}(x_A, Q^2)$ as [5]:

$$\begin{aligned} F_{2A,N}(x_A, Q^2) = & 2 \sum_{\tau=p,n} \int d^3r \int \frac{d^3p}{(2\pi)^3} \frac{M_N}{E(\mathbf{p})} \int_{-\infty}^{\mu_\tau} dp_0 S_h^\tau(p_0, \mathbf{p}, \rho^\tau(r)) \times \left(\frac{M_N}{p_0 - p_z \gamma} \right) F_{2\tau}(x_N, Q^2) \\ & \times \left[\frac{Q^2}{q_z^2} \left(\frac{|\mathbf{p}|^2 - p_z^2}{2M_N^2} \right) + \frac{(p_0 - p_z \gamma)^2}{M_N^2} \left(\frac{p_z Q^2}{(p_0 - p_z \gamma) q_0 q_z} + 1 \right)^2 \right]. \end{aligned} \quad (16)$$

Similarly, taking the xx component of the nucleon and nuclear hadronic tensors, and using $F_{1N}(x) = M_N W_{1N}(\nu, Q^2)$, we obtain $F_{1A,N}(x_A, Q^2)$ as [5]:

$$\begin{aligned} F_{1A,N}(x_A, Q^2) = & 2 \sum_{\tau=p,n} AM_N \int d^3r \int \frac{d^3p}{(2\pi)^3} \frac{M_N}{E(\mathbf{p})} \int_{-\infty}^{\mu_\tau} dp_0 S_h^\tau(p_0, \mathbf{p}, \rho^\tau(r)) \times \\ & \left[\frac{F_{1\tau}(x_N, Q^2)}{M_N} + \frac{p_x^2}{M_N^2} \frac{F_{2\tau}(x_N, Q^2)}{\nu_N} \right], \text{ where } x_N = \frac{Q^2}{2(p_0 q_0 - p_z q_z)}. \end{aligned} \quad (17)$$

Moreover, in a nucleus, the virtual photon may interact with the virtual mesons leading to the modification of the nucleon structure functions due to the additional contributions of the mesons. In the numerical calculations we have considered π and ρ mesons. To obtain the contributions of π and ρ mesons to the structure functions we follow the similar procedure as in the case of nucleon with a difference that the spectral function is now replaced by the dressed meson propagator [5, 42]. We find

that

$$F_{2A,\pi(\rho)}(x, Q^2) = -6 \times a \int d^3r \int \frac{d^4p}{(2\pi)^4} \theta(p_0) \delta Im D_{\pi(\rho)}(p) 2m_{\pi(\rho)} \left(\frac{m_{\pi(\rho)}}{p_0 - p_z \gamma} \right) \times \left[\frac{Q^2}{(q_z)^2} \left(\frac{|\mathbf{p}|^2 - (p_z)^2}{2m_{\pi(\rho)}^2} \right) + \frac{(p_0 - p_z \gamma)^2}{m_{\pi(\rho)}^2} \left(\frac{p_z Q^2}{(p_0 - p_z \gamma) q_0 q_z} + 1 \right)^2 \right] F_{2,\pi(\rho)}(x_{\pi(\rho)}, Q^2), \quad (18)$$

$$F_{1A,\pi(\rho)}(x, Q^2) = -6 \times a \times AM_N \int d^3r \int \frac{d^4p}{(2\pi)^4} \theta(p_0) \delta Im D_{\pi(\rho)}(p) 2m_{\pi(\rho)} \times \left[\frac{F_{1,\pi(\rho)}(x_{\pi(\rho)}, Q^2)}{m_{\pi(\rho)}} + \frac{|\mathbf{p}|^2 - p_z^2}{2(p_0 q_0 - p_z q_z)} \frac{F_{2,\pi(\rho)}(x_{\pi(\rho)}, Q^2)}{m_{\pi(\rho)}} \right], \quad (19)$$

where $x_{\pi(\rho)} = \frac{Q^2}{-2p \cdot q}$, $m_{\pi(\rho)}$ is the mass of pi(rho) meson and the constant factor a is 1 in the case of pi meson and 2 in the case of ρ meson [42]. $D_{\pi(\rho)}(p)$ is the meson propagator which is given by

$$D_{\pi(\rho)}(p) = [p_0^2 - \mathbf{p}^2 - m_{\pi(\rho)}^2 - \Pi_{\pi(\rho)}(p_0, \mathbf{p})]^{-1}, \quad (20)$$

where $\Pi_{\pi(\rho)}$ is the meson self energy defined in terms of the form factor $F_{\pi(\rho)NN}(p)$ and irreducible self energy $\Pi_{\pi(\rho)}^*$ as

$$\Pi_{\pi(\rho)} = \frac{\left(\frac{f^2}{m_\pi^2} \right) c'_{\pi(\rho)} F_{\pi(\rho)NN}^2(p) \mathbf{p}^2 \Pi_{\pi(\rho)}^*}{1 - \frac{f^2}{m_\pi^2} V'_j \Pi_{\pi(\rho)}^*}, \text{ where } F_{\pi(\rho)NN}(p) = \left(\frac{\Lambda^2 - m_{\pi(\rho)}^2}{\Lambda^2 + \mathbf{p}^2} \right). \quad (21)$$

In the above expression, $V'_j = V'_L(V'_T)$ for the pi(rho) meson, are the longitudinal(transverse) part of spin-isospin interaction, respectively, the expressions for which are taken from the Ref. [42] with $c'_\pi = 1$ and $c'_\rho = 3.94$, $\Lambda = 1 \text{ GeV}$ and $f = 1.01$. These parameters have been fixed in our earlier works [5, 44] while describing nuclear medium effects in the electromagnetic nuclear structure function $F_{2A}(x, Q^2)$ to explain the latest data from the JLab and other experiments performed using charged lepton scattering from several nuclear targets in the DIS region.

We now define the total EM nuclear structure functions $F_{iA}(x, Q^2)$ ($i=1,2$) which include the nuclear medium effects as:

$$F_{iA}(x, Q^2) = F_{iA,N}(x, Q^2) + F_{iA,\pi}(x, Q^2) + F_{iA,\rho}(x, Q^2); \quad i = 1, 2. \quad (22)$$

We, therefore, define $F_{LA}(x, Q^2)$, $R_A(x, Q^2)$ and $R_{2A}(x, Q^2)$ in nuclear targets in analogy with $F_{LN}(x, Q^2)$, $R_N(x, Q^2)$ and $R_{2N}(x, Q^2)$ as:

$$F_{LA}(x, Q^2) = \left(1 + \frac{4M_N^2 x^2}{Q^2} \right) F_{2A}(x, Q^2) - 2x F_{1A}(x, Q^2), \quad (23)$$

$$R_A(x, Q^2) = \frac{F_{LA}(x, Q^2)}{2x F_{1A}(x, Q^2)} = \frac{\sigma_{LA}(x, Q^2)}{\sigma_{TA}(x, Q^2)} = \left(1 + \frac{4M_N^2 x^2}{Q^2} \right) R_{2A}(x, Q^2) - 1, \text{ where } R_{2A}(x, Q^2) = \frac{F_{2A}(x, Q^2)}{2x F_{1A}(x, Q^2)}. \quad (24)$$

III. RESULTS

The numerical results for $R_A(x, Q^2)$ defined in Eq.(24) are calculated using $F_{iA,N}(x, Q^2)$, $F_{iA,\pi(\rho)}(x, Q^2)$ ($i = 1, 2$) given in Eqs.(16), (17), (18) and (19). The quark/antiquark PDFs of the nucleon have been taken from the parameterization given by the CTEQ collaboration [46] for the calculations of $F_{2N}(x, Q^2)$ which are performed in four flavor(u , d , s , and c) scheme at the next-to-leading order(NLO) [47, 48]. $F_{1N}(x, Q^2)$ has been calculated using $F_{2N}(x, Q^2)$ given in Eq.(6) and $R_N(x, Q^2)$ given by Whitlow et al. [19]. We have incorporated the target mass correction (TMC) at the nucleon level following Ref. [15]. For the pions, we have taken the parton distribution functions given by Gluck et al. [49] and for the rho mesons, we have used the same PDFs as for the pions. We have also considered the effect of shadowing following Ref. [35].

We present the theoretical results for $R_A(x, Q^2)$ in Fig.2 for ^{12}C , ^{27}Al , ^{56}Fe and ^{63}Cu and compare them with the recent experimental results from the JLab [6]. The results are also compared with the free nucleon case i.e. $R_N(x, Q^2)$ as parameterized by Whitlow et al. [19]. The results have been presented for the two cases (i) without applying any cut on the CM energy W (solid line), thus including the contributions to $R_A(x, Q^2)$ from the allowed kinematic region in W and (ii) by applying a cut on $W \geq 1.4 \text{ GeV}$ (dotted line), the case in which $R_A(x, Q^2)$ does not include the contribution from the $\Delta(1232)$ resonance region.

We observe that:

1. Our treatment of the nuclear medium effects without a cut on W (solid line) satisfactorily reproduces the experimental data for $R_A(x, Q^2)$ from the JLab [6] for $Q^2 \geq 2 \text{ GeV}^2$ but overestimates them at lower Q^2 ($Q^2 \leq 2 \text{ GeV}^2$) in the region of $x \geq 0.5$,

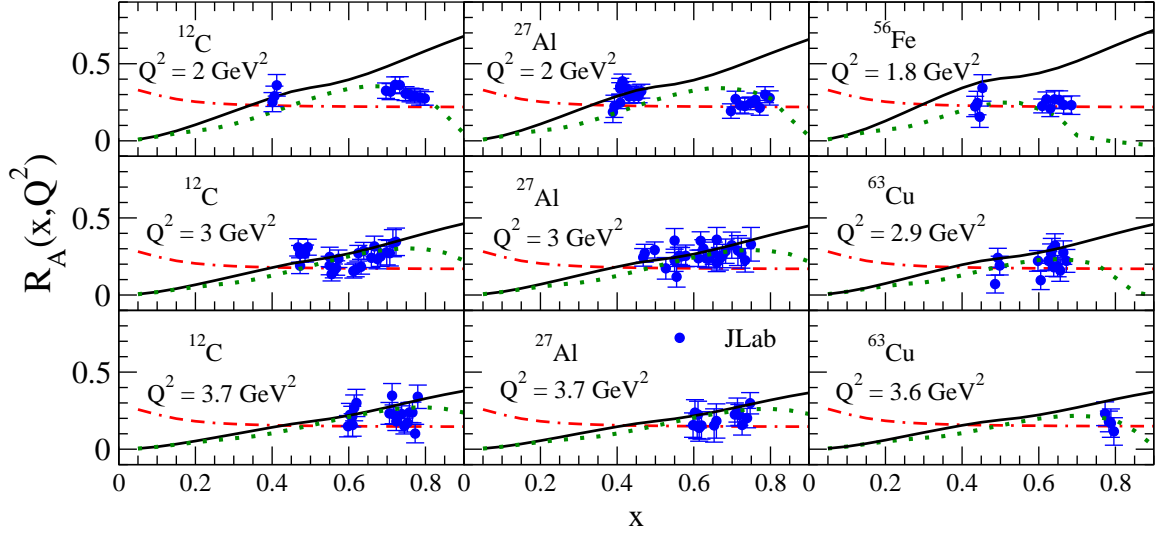


FIG. 2: $R_A(x, Q^2) = \frac{F_{LA}(x, Q^2)}{2xF_{1A}(x, Q^2)}$ ($A = {}^{12}\text{C}$, ${}^{27}\text{Al}$ (isoscalar), ${}^{56}\text{Fe}$, ${}^{63}\text{Cu}$ (nonisoscalar)) vs x are shown at different Q^2 . The results are obtained using the present model (i) without any kinematical cut on CM energy (solid line) and (ii) with a kinematical cut on CM energy $W > 1.4 \text{ GeV}$ (dotted line). The results are compared with the results for the free nucleon case obtained by using the parameterization of Whitlow et al. [19] (double dashed-dotted line) and the experimental data of the JLab (bold circles) [6].

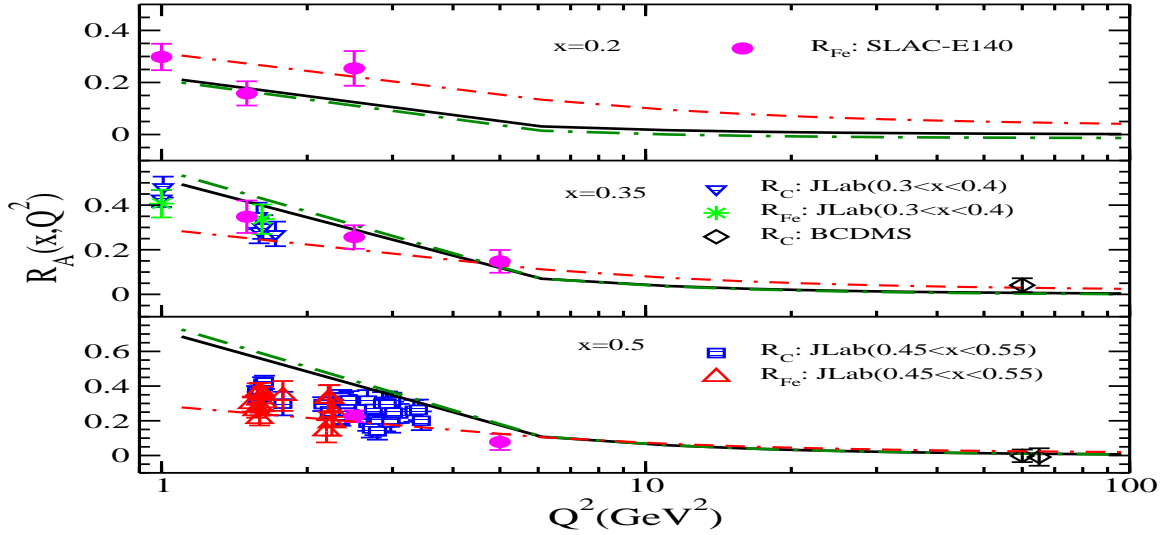


FIG. 3: $R_A(x, Q^2) = \frac{F_{LA}(x, Q^2)}{2xF_{1A}(x, Q^2)}$ ($A = {}^{12}\text{C}$ and ${}^{56}\text{Fe}$) vs Q^2 are shown at different x obtained by using the present model for isoscalar nuclear targets. Numerical results in ${}^{12}\text{C}$ (solid line) and in ${}^{56}\text{Fe}$ (dashed-dotted line) are compared with the results of free nucleon case (double dashed-dotted line) obtained by using the parameterization of Whitlow et al. [19]. The results are also compared with the experimental data from the JLab (in ${}^{12}\text{C}$ and ${}^{56}\text{Fe}$) [6], SLAC-E140 (in ${}^{56}\text{Fe}$) [23] and the BCDMS (in ${}^{12}\text{C}$) [27].

2. Our theoretical results with a cut on $W \geq 1.4 \text{ GeV}$ (dotted line) satisfactorily explain the experimental data in the entire region of $Q^2 (1 < Q^2 < 5 \text{ GeV}^2)$ and $x (0.5 < x < 0.8)$ of the JLab experiment [6].
3. The nuclear medium effects on $R_A(x, Q^2)$ show a structure with x , i.e. at lower $x (x < x_o)$ the nuclear medium effect decreases the value of $R_A(x, Q^2)$ i.e. $R_A(x, Q^2) < R_N(x, Q^2)$ while for higher $x (x > x_o)$ it increases i.e. $R_A(x, Q^2) \geq R_N(x, Q^2)$ with a cross over at $x = x_o$. The value of x_o is dependent on Q^2 and lies between 0.35 and 0.55 for $2 < Q^2 < 10 \text{ GeV}^2$. In the kinematic region of the JLab data [6] shown in Fig.2, i.e. $2 < Q^2 < 3.7 \text{ GeV}^2$ and $x \geq 0.4$, the nuclear medium effects are small without the inclusion of first resonance region ($W > 1.4 \text{ GeV}$) but are enhanced when the

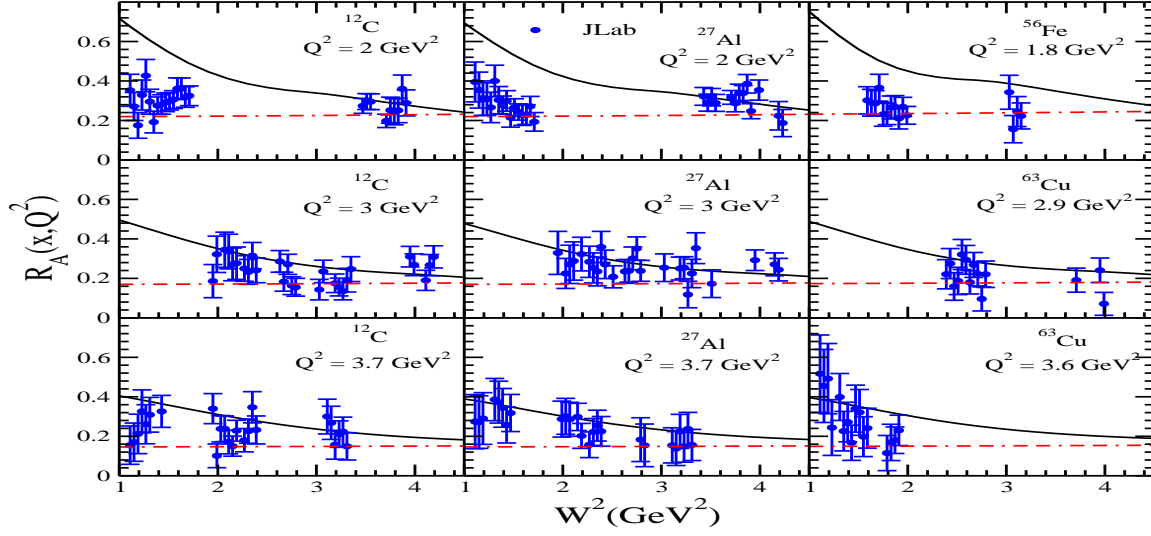


FIG. 4: Results for $R_A(x, Q^2) = \frac{F_{LA}(x, Q^2)}{2xF_{1A}(x, Q^2)}$ ($A = {}^{12}\text{C}, {}^{27}\text{Al}$ (isoscalar), ${}^{56}\text{Fe}, {}^{63}\text{Cu}$ (nonisoscalar)) vs W^2 are shown at different Q^2 . Numerical results obtained using the present model (solid line) are compared with the results of free nucleon case using the parameterization of Whitlow et al. [19] (double dashed-dotted line) and with the experimental data of the JLab [6] (bold circles).

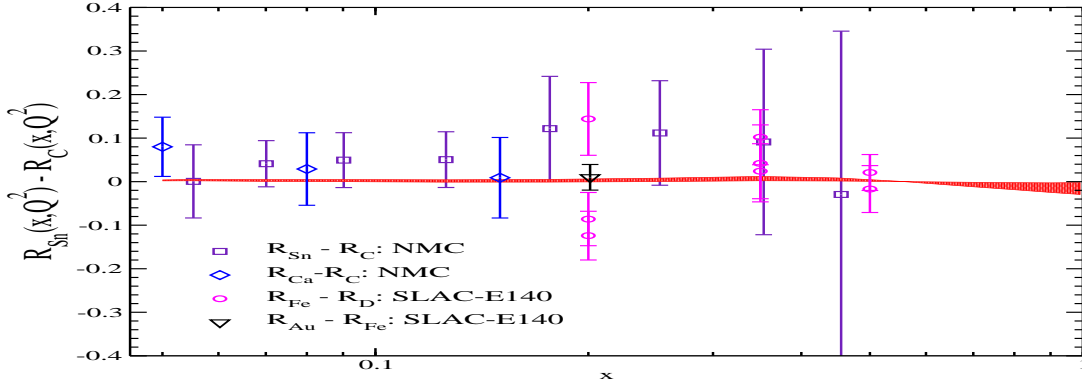


FIG. 5: Numerical results for $R_{Sn}(x, Q^2) - R_C(x, Q^2)$ vs x are obtained using the present model for $4 < Q^2 < 35 \text{ GeV}^2$ (narrow band) and the nuclear targets are treated as isoscalar. These results are compared with the experimental results for $R_{Fe}(x, Q^2) - R_D(x, Q^2)$ [23] (circle), $R_{Au}(x, Q^2) - R_{Fe}(x, Q^2)$ [23] (down triangle), $R_{Ca}(x, Q^2) - R_C(x, Q^2)$ [39] (diamond) and $R_{Sn}(x, Q^2) - R_C(x, Q^2)$ [40] (square).

contribution of the first resonance region (without cut on W) is also included. In both the cases (with or without cut on W), the nuclear medium effects decrease with Q^2 and have almost no dependence on the mass number A . The above observations imply that:

- In the region of $Q^2 \leq 2 \text{ GeV}^2$, our results of $R_A(x, Q^2)$ are larger than the experimental data. These results are obtained using the DIS formalism in the entire kinematic region which includes the first resonance region (i.e. $1.3 \text{ GeV}^2 < W^2 < 1.9 \text{ GeV}^2$) dominated by $\Delta(1232)$ and possibly $N^*(1440)$ resonance. A comparison of our results with and without cut of W suggests that in the kinematic region of $Q^2 < 2 \text{ GeV}^2$, the use of DIS formalism is not appropriate and a calculation of $R_A(x, Q^2)$, using explicit mechanism for $\Delta(1232)$ and $N^*(1440)$ resonance excitations in the nuclear medium would give a better description of $R_A(x, Q^2)$.
- The contribution to $R_A(x, Q^2)$ from the resonance region is also well reproduced by the DIS formalism at high Q^2 . This supports the conclusion drawn from the study of Bloom-Gilman duality in the free nucleon case, that the quark-hadron (QH) duality works better in the higher resonance region than in the region of $\Delta(1232)$ resonance [14] as our results for $R_A(x, Q^2)$ using DIS formalism seem to agree better with the experimental results in the higher Q^2 region than in the lower Q^2 region specially for $x \geq 0.5$.

Our theoretical results are also in agreement with the results of $R_A(x, Q^2)$ reported from the SLAC E140 [23] and

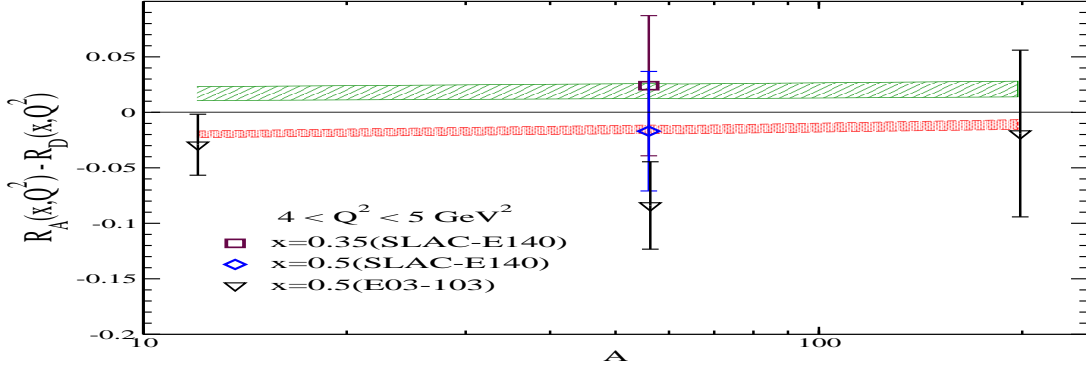


FIG. 6: Results for $R_A(x, Q^2) - R_D(x, Q^2)$ vs A obtained using the present model are presented for ^{12}C , ^{56}Fe , ^{63}Cu and ^{197}Au in the range of $4 < Q^2 < 5 \text{ GeV}^2$ for $x = 0.4$ (lower band) and $x = 0.5$ (upper band). The results are compared with the experimental results of the JLab [3] and the SLAC-E140 [23] corresponding to the x values shown in the figure. Nuclear targets are treated as isoscalar.

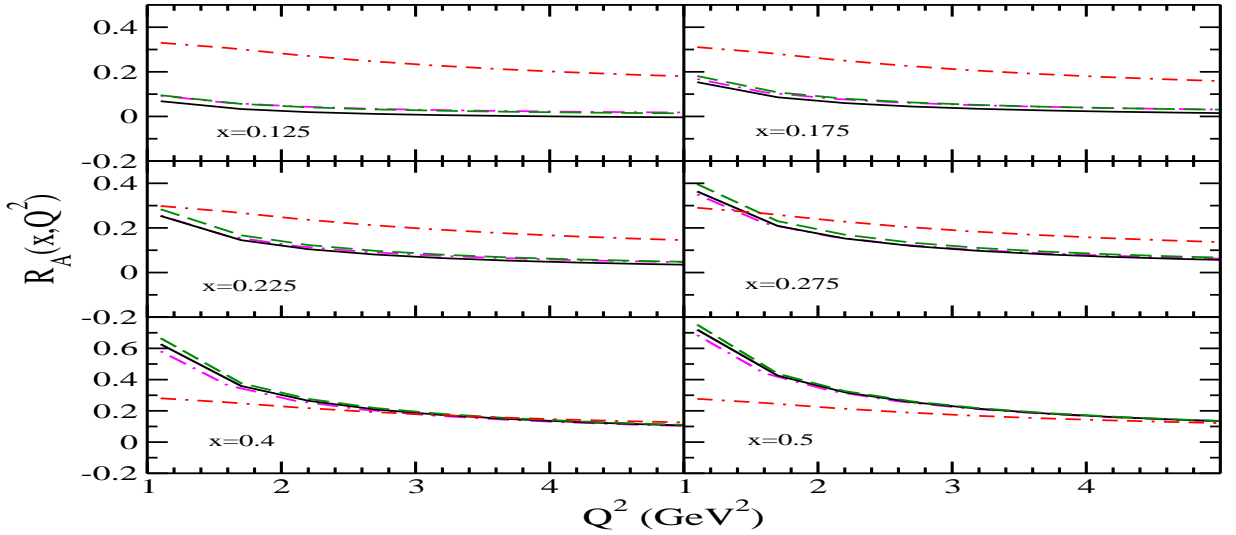


FIG. 7: Results for $R_A(x, Q^2)$ vs Q^2 obtained using the present model are shown at different x for some nuclei viz. ^{12}C (dashed-dotted line), ^{63}Cu (solid line) and ^{197}Au (dashed line). The results are compared with the results of free nucleon case obtained by using the parameterization of Whitlow et al. [19] (double dashed-dotted line). Nuclear targets are treated as isoscalar.

BCDMS [27] experiments as shown in Fig.3 at the different values of x and Q^2 in ^{12}C and ^{56}Fe . From the figure it may be observed that the present theoretical results are in agreement with the results of BCDMS experiment [27] at high Q^2 but overestimate the SLAC E140 results [23] at lower Q^2 for $x \geq 0.5$. These results also show that the CGR is satisfied in the case of nuclei i.e. $R_A(Q^2) \rightarrow 0$ at high Q^2 at the same level of precision as in the case of free nucleon for $0.2 \leq x \leq 0.5$. At lower Q^2 , the deviation from the free nucleon case, i.e. $R_N(x, Q^2)$ is in the right direction to explain the experimental data but overestimate them.

In order to further discuss the results presented in Fig.2 and Fig.3 above, we have shown in Fig.4, the values of $R_A(x, Q^2)$ vs W^2 for the various values of Q^2 . We find that at higher Q^2 ($Q^2 > 2 \text{ GeV}^2$), our results are in fair agreement with the experimental data for $W^2 \leq 4 \text{ GeV}^2$ obtained from the JLab [6] in ^{12}C , ^{27}Al , ^{56}Fe , and ^{63}Cu . However, at lower Q^2 ($Q^2 \leq 2 \text{ GeV}^2$), the theoretical results using DIS formalism overestimate $R_A(x, Q^2)$ for $W^2 < 2.5 \text{ GeV}^2$ which describes the resonance region dominated by the $\Delta(1232)$ and $N^*(1440)$ resonances. This strengthens our assertion that in the region of low Q^2 and W^2 a realistic calculation of $R_A(x, Q^2)$ using explicitly the $\Delta(1232)$ and $N^*(1440)$ resonance excitations in the nuclear medium should be more appropriate than the use of DIS formalism. The theoretical results obtained using the present model for $R_A(x, Q^2)$ for all the nuclei shown in Fig.4 are in better agreement with the experimental results when the nuclear medium effects are included specially in the region of $W^2 \geq 2.5 \text{ GeV}^2$ for all Q^2 considered here. We also observe that the effect of nuclear medium leads to an enhancement in the value of $R_A(x, Q^2)$ over $R_N(x, Q^2)$ in the region of W^2 considered here. This enhancement is quite small at higher W^2 but is large at lower W^2 . It decreases with the increase in Q^2 and is almost independent of A .

The world data on nuclear dependence of $R_A(x, Q^2)$ have been compiled and reanalyzed by Guzey et al. [2] and Solvignon et al. [3]. We show in Fig.5, a comparison of our present results with the experimental data summarized by Guzey et al. [2]. A reasonable agreement with the experimental data [23, 39, 40] is seen for $R_A(x, Q^2) - R_{A'}(x, Q^2)$ for A and A' nuclei as shown in Fig.5. Our results are also in agreement with the recent experimental results from the JLab [6] for $R_A(x, Q^2) - R_C(x, Q^2)$ for $A = {}^{27}\text{Al}$ and ${}^{63}\text{Cu}$ which are not reproduced here as they have very large uncertainties due to systematic and statistical errors. We also show the A dependence of $R_A(x, Q^2) - R_D(x, Q^2)$ in Fig.6 and compare it with the data of JLab [3] and SLAC [23]. We find that $R_A(x, Q^2) - R_D(x, Q^2)$ is negative for $x < 0.45$ and changes sign for $x > 0.45$ and it has almost no dependence on A in the absence of Coulomb effects which are not considered in this work.

A precise determination of the structure functions in nuclei using the method of Rosenbluth separation requires a knowledge of $R_A(x, Q^2)$ with high accuracy. An experiment to measure the nuclear dependence of $R_A(x, Q^2)$ and to determine the structure functions $F_{1A}(x, Q^2)$, $F_{2A}(x, Q^2)$ and $F_{LA}(x, Q^2)$ with high precision in ${}^{12}\text{C}$, ${}^{63}\text{Cu}$ and ${}^{197}\text{Au}$ nuclei has been proposed at the JLab [9] in the kinematic region of $0.1 < x < 0.6$ and $1 < Q^2 < 5 \text{ GeV}^2$ for W^2 up to 10 GeV^2 . We, therefore, show in the Fig.7 the results of $R_A(x, Q^2)$ vs Q^2 for various values of x using the present model relevant for the kinematics of the JLab experiment [9].

A comparison of our results with the experimental results of the JLab experiment [9] in the future will help to obtain a more precise determination of the nuclear structure functions and provide further insight in understanding the physics of the nuclear medium effects in the DIS of the electrons from nuclear targets.

IV. SUMMARY

We have in this work studied the nuclear medium effects on the ratio $R_A(x, Q^2) = \frac{F_{LA}(x, Q^2)}{2xF_{1A}(x, Q^2)}$ and its impact on the Callan-Gross relation (CGR) in nuclei, using a microscopic nuclear model and considered the effects of the Fermi motion, binding energy, nucleon correlations, mesonic contribution and shadowing. We find that

- The inclusion of nuclear medium effects leads to a better description of the experimental data from JLab[6], SLAC [23], BCDMS [27] and NMC [39, 40] in various nuclei in a wide range of x and Q^2 . At high Q^2 the experimental results are well reproduced, while at low Q^2 ($\leq 2 \text{ GeV}^2$) we overestimate the experimental data for $x \geq 0.5$.
- In nuclei, the Callan-Gross relation is satisfied at high Q^2 with almost the same precision as in the case of free nucleon for all the values of x . At lower and moderate Q^2 , there is deviation in $R_A(x, Q^2)$ from the free nucleon value due to the nuclear medium effects and it is in the right direction to give a better description of the available experimental data but overestimates them for $x > 0.2$.
- With the inclusion of nuclear medium effects, $R_A(x, Q^2)$ is almost independent of A for $A \geq 12$ subject to the Coulomb corrections which are small and relevant only for the DIS of the low energy electrons from high Z nuclear targets.
- The use of DIS formalism to calculate the contribution of $R_A(x, Q^2)$ in the region of low W^2 and low Q^2 overestimates the experimental results in this region. In this kinematic region an explicit calculation of $R_A(x, Q^2)$ arising due to the resonance excitation of $\Delta(1232)$ and $N^*(1440)$ in the nuclear medium should be more appropriate. This also indicates that the phenomenon of QH duality in nuclei works better in the kinematic region beyond the first resonance region as in the case of the free nucleon.

-
- [1] A. Bodek, PoS DIS **2015**, 026 (2015).
 - [2] V. Guzey *et al.*, Phys. Rev. C **86**, 045201 (2012).
 - [3] P. Solvignon *et al.*, AIP Conf. Proc. **1160**, 155 (2009).
 - [4] K. Kovarik *et al.*, Phys. Rev. Lett. **106**, 122301 (2011).
 - [5] H. Haider *et al.*, Nucl. Phys. A **955**, 58 (2016); Nucl. Phys. A **943**, 58 (2015).
 - [6] V. Mamyan, arXiv:1202.1457 [nucl-ex].
 - [7] <https://www.jlab.org/12GeV/>.
 - [8] <https://www.jlab.org/exp-prog/experiments>.
 - [9] S. Covrig *et al.* <https://www.jlab.org/exp-prog/proposals/14/PR12-14-002.pdf>.
 - [10] <http://www.fnal.gov/pub/science/particle-physics/experiments/neutrinos.html>.
 - [11] J. Mousseau *et al.* [MINERvA Collaboration], Phys. Rev. D **93**, no. 7, 071101 (2016).
 - [12] C. G. Callan, Jr. and D. J. Gross, Phys. Rev. Lett. **22**, 156 (1969).
 - [13] R. Devenish and A. C. Sarkar “Deep Inelastic Scattering”, Oxford University Press, Edition (2008).
 - [14] W. Melnitchouk *et al.*, Phys. Rept. **406**, 127 (2005).
 - [15] I. Schienbein *et al.*, J. Phys. G **35**, 053101 (2008).
 - [16] P. Castorina and P. J. Mulders, Phys. Rev. D **31**, 2753 (1985).
 - [17] W. Melnitchouk, Nucl. Phys. A **782**, 126 (2007).
 - [18] J. L. Miramontes, M. A. Miramontes and J. Sanchez Guillen, Phys. Rev. D **40**, 2184 (1989).

- [19] L. W. Whitlow *et al.*, Phys. Lett. B **250**, 193 (1990); Phys. Lett. B **282**, 475 (1992).
- [20] A. Bodek and U. K. Yang, arXiv:1011.6592 [hep-ph]; Nucl. Phys. Proc. Suppl. **112**, 70 (2002).
- [21] M. E. Christy and P. E. Bosted, Phys. Rev. C **81**, 055213 (2010).
- [22] K. Abe *et al.* [E143 Collaboration], doi:10.1016/S0370-2693(99)00244-0 [hep-ex/9808028].
- [23] S. Dasu *et al.*, Phys. Rev. Lett. **61**, 1061 (1988); Phys. Rev. D **49**, 5641 (1994); Phys. Rev. Lett. **60**, 2591 (1988).
- [24] V. Tvaskis *et al.*, Phys. Rev. Lett. **98**, 142301 (2007).
- [25] P. Monaghan *et al.*, Phys. Rev. Lett. **110**, no. 15, 152002 (2013).
- [26] Y. Liang *et al.* [Jefferson Lab Hall C E94-110 Collaboration], nucl-ex/0410027.
- [27] A. C. Benvenuti *et al.* [BCDMS Collaboration], Phys. Lett. B **223**, 485 (1989); Phys. Lett. B **195**, 91 (1987).
- [28] J. J. Aubert *et al.* [European Muon Collaboration], Phys. Lett. B **123**, 275 (1983).
- [29] A. Bodek *et al.*, Phys. Rev. Lett. **50**, 1431 (1983); Phys. Rev. Lett. **51**, 534 (1983).
- [30] D. F. Geesaman *et al.*, Ann. Rev. Nucl. Part. Sci. **45**, 337 (1995).
- [31] S. Malace *et al.*, Int. J. Mod. Phys. E **23**, 1430013 (2014).
- [32] O. Hen, D. W. Higinbotham, G. A. Miller, E. Piasetzky and L. B. Weinstein, Int. J. Mod. Phys. E **22**, 1330017 (2013).
- [33] P. Castorina, Phys. Rev. D **65**, 097502 (2002).
- [34] G. A. Miller, S. J. Brodsky and M. Karliner, Phys. Lett. B **481**, 245 (2000).
- [35] S. A. Kulagin and R. Petti, Nucl. Phys. A **765**, 126 (2006).
- [36] M. Ericson and S. Kumano, Phys. Rev. C **67**, 022201 (2003).
- [37] N. Armesto *et al.*, Phys. Lett. B **694**, 38 (2011).
- [38] J. Gomez *et al.*, Phys. Rev. D **49**, 4348 (1994).
- [39] P. Amaudruz *et al.* [New Muon Collaboration], Phys. Lett. B **294**, 120 (1992).
- [40] M. Arneodo *et al.* [New Muon Collaboration], Nucl. Phys. B **481**, 23 (1996).
- [41] P. Fernandez de Cordoba and E. Oset, Phys. Rev. C **46**, 1697 (1992).
- [42] E. Marco *et al.*, Nucl. Phys. A **611**, 484 (1996).
- [43] C. Garcia-Recio *et al.*, Phys. Rev. C **51**, 237 (1995).
- [44] H. Haider *et al.*, Nucl. Phys. A **940**, 138 (2015); Phys. Rev. C **84**, 054610 (2011); Phys. Rev. C **85**, 055201 (2012); *ibid* Phys. Rev. C **87**, 035502 (2013); M. Sajjad Athar *et al.*, Nucl. Phys. A **857**, 29 (2011).
- [45] H. Haider *et al.*, J. Phys. G **44**, 045111 (2017).
- [46] Pavel M. Nadolsky *et al.*, Phys. Rev. D **78**, 013004 (2008); <http://hep.pa.msu.edu/cteq/public>.
- [47] J. A. M. Vermaseren *et al.*, Nucl. Phys. B **724**, 3 (2005).
- [48] W. L. van Neerven and A. Vogt, Nucl. Phys. B **568**, 263 (2000); *ibid* **588**, 345 (2000).
- [49] M. Gluck *et al.*, Z. Phys. C **53**, 651 (1992); Eur. Phys. J. C **10**, 313 (1999).